Corrosion protection of AA2024 sealed anodic layers using the hydrophobic properties of carboxylic acids

Grégory Boisier [a], Alain Lamure [a], Nadine Pébère [a,*], Nicolas Portail [a], Martine Villatte [b]

[a] Université de Toulouse, CIRIMAT, UPS/INPT/CNRS, ENSIACET, 118 route de Narbonne, 31077 Toulouse cedex 04, France
[b] EADS IW, 12 rue Pasteur, BP76, 92152 Suresnes cedex, France

A B S T R A C T

The present study investigates the use of carboxylic acids as a post-treatment for sealed AA2024 anodised in tartaric–sulphuric acid electrolyte. Four monocarboxylic acids with different carbon chain lengths were tested ($(CH_3–(CH_2)_n–COOH$ with $n=4$, 8, 12 and 16). Hydrophobic surface properties after the post-treatment were characterized by contact angle measurements. Electrochemical impedance spectroscopy (EIS) was performed to assess the ability of the four carboxylic acids to form protective films. It was shown that stearic acid ($n=16$) used in its pure molten state was the most efficient. The organic film formed very rapidly (under 5 min) and contributed to the enhancement of the protection in terms of corrosion resistance of the sealed anodic layers. EIS measurements showed the presence of the organic films on the specimen surface.

Keywords:
Anodic layer
Post-treatment
Carboxylic acids
Organic film
EIS

1. Introduction

In the aeronautic industry, the corrosion protection of structural aluminium alloys, such as the 2XXX and 7XXX series, requires different surface treatments which involve the use of Cr(VI) to obtain high corrosion resistance. For example, anodising of aluminium alloys is usually performed in chromic acid electrolyte and is often followed by sealing in potassium dichromate solution to improve the corrosion resistance. Since the beginning of the 1990s, the high toxicity associated with Cr(VI) has imposed restrictions on its use in industrial applications and as a consequence, this has led to the development of Cr(VI)-free surface treatments. During the last decade, attention to sulphuric acid anodising (SAA) to replace chromic acid anodising (CAA) has increased and numerous attempts have been made with new additives in the anodising bath such as molybdate, permanganate anions or cerium IV [1,2], boric acid [3–5] or tartaric acid [6]. Cr(VI)-free sealing has also been investigated. The use of sealing products such as rare earth metal salts [7], nickel acetate [8] or triethanolamine [9] has been reported. However, despite the promising performances of these new procedures, they still require further improvements to offer the same level of protection as CAA and Cr(VI) sealing.

The present paper describes a new way to strengthen the corrosion resistance of AA2024 sealed anodic layers. It consists of an additional step to anodising and sealing involving the use of carboxylic acids as a final surface treatment, called in the present study “post-treatment”. Monocarboxylic acids ($CH_3–(CH_2)_n–COOH$) are environmentally friendly and are known to act as corrosion inhibitors for various metals such as copper [10], lead [11], mild steel [12–14] aluminium alloys [15], and magnesium alloys [16]. Their action is characterised by the adsorption of the carboxylate group (negatively charged) on the metal surface (positively charged [17,18]) allowing the formation of a hydrophobic film which provides the corrosion protection. The hydrophobic characteristics of the monocarboxylic acids depend strongly on their carbon chain length [14–16]. Moreover, Landry et al. [19] showed that carboxylic acids can easily react with aluminium hydroxide (boehmite) to form alumoxanes (Al–OOC–R) which are insoluble and adhere to the surface. Shulman and Bauman [20] have used long-chain organic acids (stearic and isostearic acids) to seal anodic films formed on aluminium alloys of the 2XXX, 6XXX and 7XXX series. They showed that the organic acids protect the alloys by reacting with the outer layer of the anodic film to form “aluminium soap”. This inhibitive film renders the surface water repellent and significantly enhances salt spray resistance compared to untreated specimens. The term “aluminium soap” is used to take into account the hydrophobic character of the alumoxanes due to the long hydrocarbon chain.

The present study focussed on a surface post-treatment using the hydrophobic properties of monocarboxylates. The post-treatment was applied on AA2024 specimens anodised in tartaric–sulphuric acid (TSA) electrolyte and sealed in boiling water (hydrothermal sealing). In a recent paper [21], the beneficial effect of tartaric acid addition to the sulphuric acid bath to improve the corrosion resistance of the anodic layers was demonstrated. This effect was clearly shown after hydrothermal sealing. The morphology of the unsealed and hydro–thermally sealed anodic layers, before and after the post-treatment, was examined using field emission-scanning electron microscopy (FE-SEM). The modification of the hydrophobic surface properties after

Corresponding author. Tel.: +335 6288 5665; fax: +335 6288 5663.
E-mail address: Nadine.Pebere@ensiacet.fr (N. Pébère).

the post-treatment was characterized by contact angle measurements. Electrochemical impedance spectroscopy (EIS) was carried out first to assess the ability of the carboxylic acids to form protective films and also to characterise the corrosion behaviour of the post-treated specimens. Many studies have proved that EIS is a sensitive method that can be successfully applied to characterize the barrier and the porous layers of anodised aluminium and its alloys [22–31]. Finally, salt spray tests were performed to verify the protection afforded by the post-treatment.

2. Experimental

2.1. Material and surface treatments

The material used was a 2024 T3 aluminium alloy. The average chemical composition of the alloy is given in Table 1. The specimens consisted of 125 × 80 × 1.6 mm plates machined from an AA2024 T3 rolled plate. Before anodising, the samples were degreased at 60 °C (pH = 9) for 15 min then etched in an acid bath at 35 °C for 10 min (ARDROX®295GD). Anodising treatment was performed in a 40 g L^{-1} (0.41 M) sulphuric acid (H_2SO_4) solution in the presence of 80 g L^{-1} (0.53 M) of tartaric acid ($C_4H_6O_6$). Anodising experiments were carried out at a constant cell voltage of 14 V for 20 min reached after a 5 min voltage ramp. The operating temperature was fixed at 37 °C. Sealing was carried out in deionised water (ρ > 1500 kΩ cm) for 30 min at a temperature of over 96 °C.

2.2. Post-treatment conditions

Four different carboxylic acids (purchased from Merck) were used for the post-treatment:

- Hexanoic acid (CH_3–$(CH_2)_4$–COOH)
- Decanoic acid (CH_3–$(CH_2)_8$–COOH)
- Myristic acid (CH_3–$(CH_2)_{12}$–COOH)
- Stearic acid (CH_3–$(CH_2)_{16}$–COOH)

The carboxylic acids were used pure or in dilute solution with ethanol as solvent due to their poor solubility in water. The operating temperature was fixed at 75 °C allowing the melting of all the carboxylic acids studied. The bath was open to air without stirring. The post-treatment time was between 5 and 60 min. The excess of acid was removed by rinsing the surface with ethanol. Finally, the specimens were dried at room temperature to allow residual ethanol to evaporate off.

2.3. Field-emission scanning electron microscope observations

The morphology of the sealed or unsealed anodised specimens before and after the post-treatment was investigated using a JEOL JSM 6700F. The samples were coated with a 1 nm thick layer of platinum to reduce the charging effect on the surface and thus to improve image quality.

2.4. Contact angle measurements

The contact angles were measured using a Digidrop Contact Angle Meter from GBX Scientific Instruments. The protocol used consists in depositing a liquid drop of an accurate volume (3–5 μL) at the surface of the sample and then in measuring the static contact angle (θ). A high resolution camera and software were used to capture and analyze the contact angle. The contact angle was obtained by calculating the slope of the tangent to the drop at the liquid–solid interface. An accurate value of the angle (±1°) was given by the software. In the present study, a few seconds were sufficient to obtain stabilization of the interfacial forces and thus, the static contact angle was measured just after deposition of the liquid drop. In order to assess the homogeneity of the surface properties, 20 measurements were performed on different locations on the samples and the average contact angle was calculated. Deionised water was used as liquid for the droplets to evaluate the hydrophilic (θ<90°) or hydrophobic (θ>90°) character of the surface. All the experiments were performed at room temperature and constant humidity (~50%).

Table 1
Chemical composition (in weight percent) of 2024 T3 aluminium alloy.

Cu	Mg	Mn	Si	Fe	Zn	Ti	Al
4.50	1.44	0.60	0.06	0.13	0.02	0.03	Bal.

2.5. Electrochemical experiments

A three-electrode electrochemical cell was used. It contained a platinum grid as auxiliary electrode and the untreated or post-treated anodised AA2024 T3 specimens as working electrode (exposed area of 28 cm^2). A saturated sulphate reference electrode (SSE) was used in Na_2SO_4-containing solution and a saturated calomel reference electrode (SCE) was used in NaCl-containing solution. Electrochemical impedance measurements were carried out using a Solartron 1287 electrochemical interface and a Solartron 1250 frequency response analyser. The impedance diagrams were plotted under potentiostatic conditions at the corrosion potential over a frequency range of 65 kHz to 10 mHz with 6 points per decade using a 20 mV peak-to-peak sinusoidal voltage. The electrochemical cell was kept at room temperature and open to air. The electrochemical properties of the specimens were characterised after 2 h of immersion in a 0.5 M Na_2SO_4 solution. Sodium sulphate was chosen for its low corrosiveness toward aluminium and aluminium alloys. The corrosion behaviour of carboxylate post-treated specimens was investigated in a 0.5 M NaCl solution, at different exposure times reaching 35 days (840 h). Fitting of the impedance spectra was performed using Zview software (Scribner Associates Inc.).

2.6. Salt spray test

Salt spray tests were performed according to ISO9227. A solution of 5% NaCl was sprayed on the samples in a closed testing chamber (T = 35 °C). The spraying was maintained for the duration of the test. After different exposure times, the maximum being 672 h, the samples were observed and the number of corrosion points was determined.

3. Results and discussion

3.1. FE-SEM observations

Fig. 1 presents the FE-SEM micrographs of the surface of the unsealed (Fig. 1a) and hydrothermally sealed (30 min of sealing in boiling water) (Fig. 1b) anodic layers. Before sealing (Fig. 1a), the porous structure of the anodic layer is clearly observable. The pores are well distributed and have an average diameter close to 10 nm. After hydrothermal sealing (Fig. 1b), the surface appears strongly modified. The initial porous structure has disappeared and a layer of "petal-shaped" crystals covers the entire surface. The formation of these petal-shaped crystals on the surface, so-called "smudge" is the result of aluminium salt precipitation occurring during the sealing reaction [32,33]. FE-SEM observations of both post-treated unsealed and hydrothermally sealed anodic layers (not shown) were identical to those presented in Fig. 1a and b. This can be explained either by the fact that the organic film was very thin and not observable by FE-SEM or by the fact that the organic film could have been deteriorated ("burnt") by the high-energy electron beam.

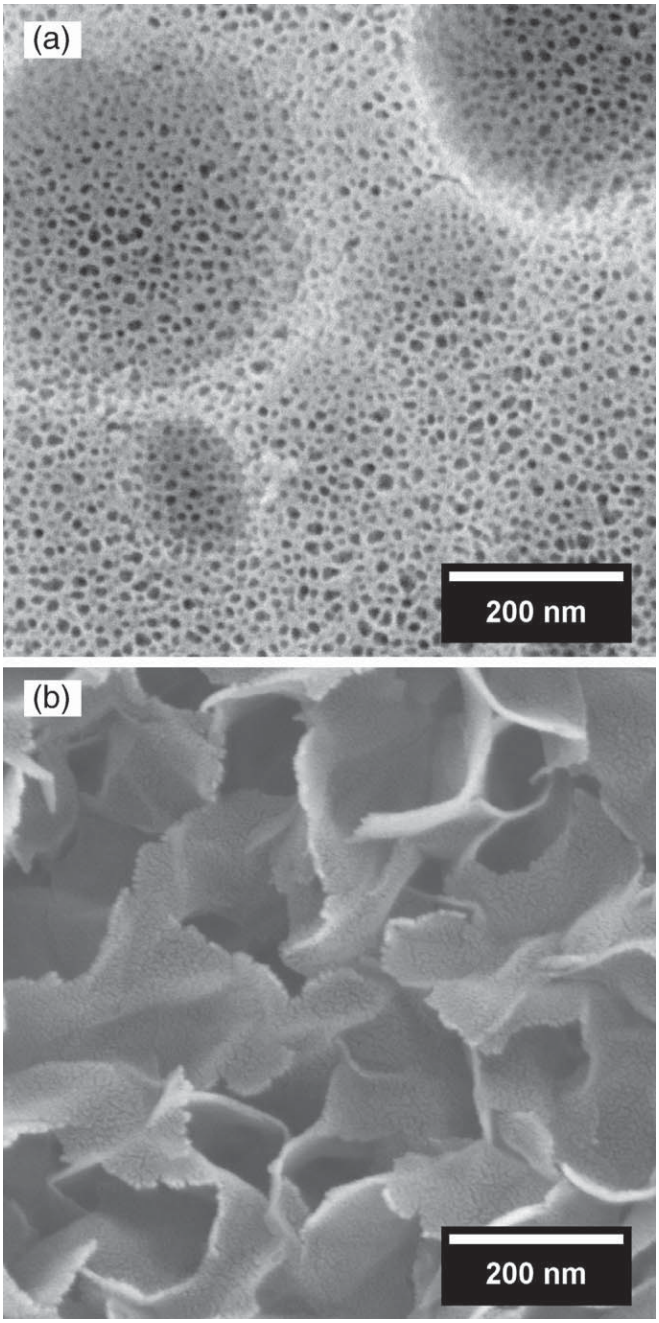

Fig. 1. FE-SEM observations of the surface of (a) unsealed and (b) 30 min sealed anodic layers formed in tartaric–sulphuric acid electrolyte.

The anodic layer thickness, measured from SEM observations of cross-sections, was 2.4 μm and 2.6 μm for the unsealed and sealed layers, respectively.

3.2. Influence of the carboxylic acid concentration

The influence of the carboxylic acid concentration was investigated by measuring the average contact angles after post-treatment. Fig. 2 presents the results obtained for sealed specimens treated for 30 min at 75 °C in solutions containing the decanoic acid ($n = 8$) at different concentrations (0.05 M, 0.29 M and pure molten). Before post-treatment, the contact angle was about 10° revealing the high hydrophilic character of the sealed anodic layer. In contrast, when the post-treatment was applied, a significant increase of the contact angle was observed. In addition, the higher the carboxylic acid concentration, the higher the contact angle. The best result was obtained when the decanoic acid was used in its pure molten state. The contact angle value was then around 110°. These results clearly confirm that the carboxylic acids can react with the aluminium hydroxide of sealed anodic layers to form an organic film (alumoxane type) which presents strong hydrophobic properties, particularly when the acid is used in its pure molten state. Thus, in the reminder of the study, the post-treatment was carried out only with pure molten carboxylic acids.

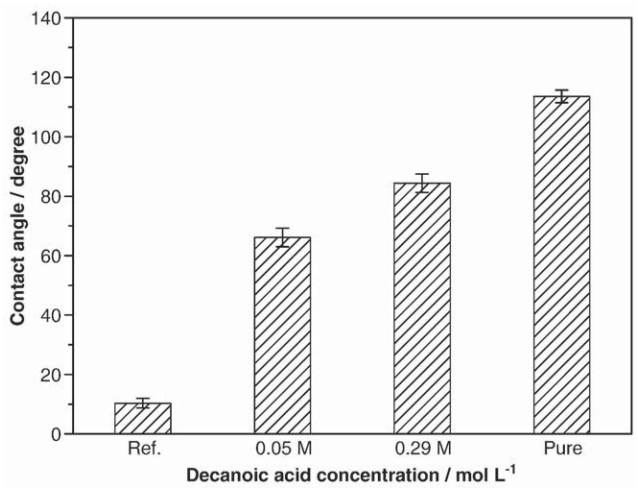

Fig. 2. Contact angles measured on the surface of sealed anodic layers untreated or post-treated for 30 min at 75 °C in a solution containing decanoic acid: 0.05 M in ethanol, 0.29 M in ethanol and pure molten.

3.3. Influence of the carbon chain length

The influence of the carbon chain length, *n*, on the post-treatment efficiency was also evaluated by the measurements of the contact angles on sealed specimens treated for 30 min at 75 °C in pure molten acids (Fig. 3). It can be observed that the hydrophobic character was less pronounced when the post-treatment was performed with hexanoic acid ($n = 4$): the contact angle was around 50°. This suggests that the carbon chain of hexanoic acid is not long enough to confer a hydrophobic effect. In contrast, for the three other post-treated specimens the contact angle value was between 110 and 120°. This shows that the post-treated anodic layer had a strong hydrophobic

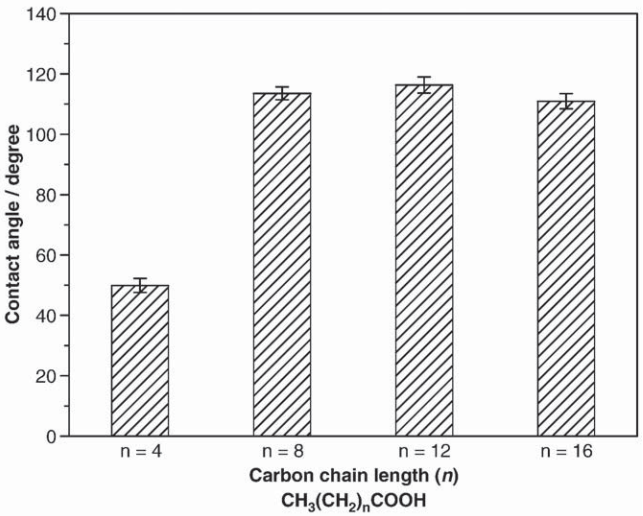

Fig. 3. Contact angles measured on the surface of sealed anodic layers after post-treatment for 30 min at 75 °C in pure molten carboxylic acids of different carbon chain lengths.

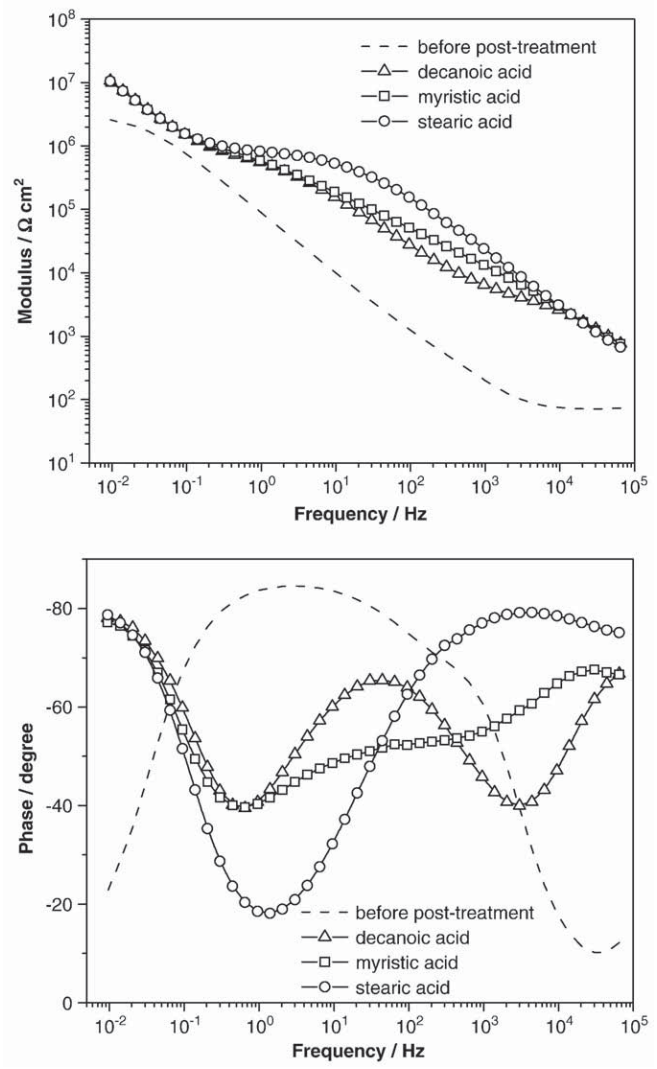

Fig. 4. Bode plots of unsealed anodic layers obtained before or after post-treatment for 30 min at 75 °C in pure molten acids (diagrams plotted after 2 h of immersion in 0.5 M Na_2SO_4).

character but the contact angle measurements did not allow differences to be observed between the efficiency of post-treatments with $n=6$, 8 and 12 carboxylic acids. Thus, we performed impedance measurements after 2 h of immersion in sodium sulphate solution to investigate the transformations induced by the post-treatment. From these data, it was again not possible to discriminate between the efficiency of the different carboxylic acids ($n>6$). This can be explained by the fact that the impedance response is mainly governed by the properties of the sealed anodic layers which conferred a high resistance to the system (the results are not reported here for the sake of simplicity). For this reason, post-treatment with the three carboxylic acids ($n=8$, 12, 16) was analysed on unsealed specimens. The impedance diagrams were therefore characterised by lower resistances both in the high and the low frequency ranges [21].

Table 2
Fitted values of the parameters associated to the high-frequency part of the impedance diagrams of unsealed anodic layers post-treated for 30 min at 75 °C in pure molten carboxylic acids of different carbon chain lengths (diagrams obtained after 2 h of immersion in 0.5 M Na_2SO_4).

N	R_f (kΩ cm^2)	Q_f (MΩ^{-1} cm^{-2} s$^{\alpha}$)	α_f
8	5	25	0.84
12	10	20	0.87
16	300	16	0.90

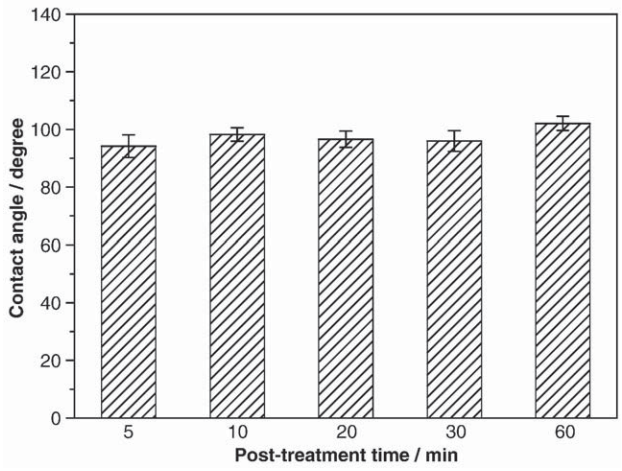

Fig. 5. Contact angles measured on the surface of sealed anodic layers after post-treatment for 5 to 60 min at 75 °C in pure molten stearic acid.

The impedance diagrams obtained for the unsealed anodic layers before and after the post-treatment, after 2 h of immersion in a 0.5 M Na_2SO_4 solution, are presented in Fig. 4. For the untreated anodic layer, a time constant is observable in the medium frequency range (1 kHz)

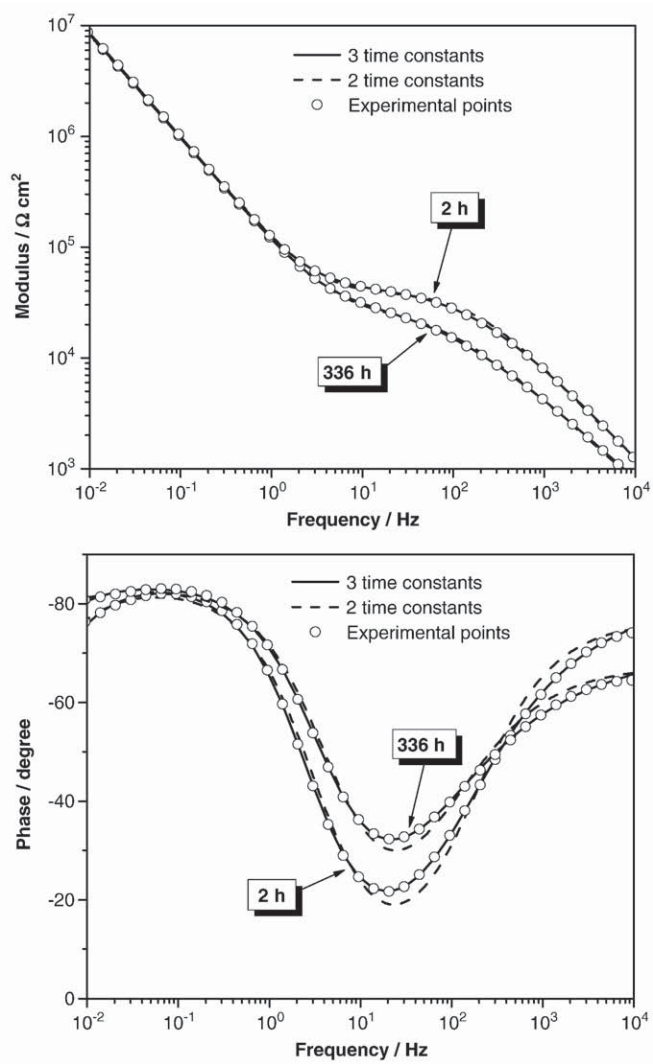

Fig. 6. Bode plots of sealed anodic layers obtained after post-treatment for 60 min at 75 °C in pure molten stearic acid (diagrams plotted after 2 h and 336 h of immersion in 0.5 M NaCl). Results fitted with 3 or 2 time constants.

attributed to the response of the pore walls of the anodic layer [21]. The time constant located in the low-frequency part of the diagrams is attributed to the barrier layer response [22,31]. For the post-treated specimens, the diagrams present a new time constant located in the high frequency range (10^4 Hz) which is assumed to represent the response of the hydrophobic film covering the surface. The presence of the organic film is clearly demonstrated in the next section. A second time constant is also observable in the medium frequency range. In this case, it is possible that the carboxylic acids penetrated through the porous structure of the anodic layer during the post-treatment, as suggested by Shulman and Bauman [20], and were thus able to react with the alumina. Consequently, the formation of alumoxanes partially closed the pores in a way analogous to hydrothermal sealing. These transformations are reflected in the medium frequency range of the diagrams. The time constant located in the low-frequency part of the diagrams is always attributed to the barrier layer response.

From the high frequency part of the impedance spectra (65 kHz–600 Hz), the parameters associated to the hydrophobic film on the surface can be extracted by using a simple equivalent circuit: a resistance, R_f, representing the electrolyte resistance through the film (pores) and a capacitance representing the properties of the film. A constant phase element (CPE) was introduced instead of a pure capacitance (Q_f, α_f), in order to take into account the non-ideal behaviour of the film [34]. The fitted parameters are reported in Table 2. The resistance R_f increased with the n values whereas the value of Q_f remained relatively constant. This could be because the film thickness does not vary significantly, whereas penetration through the film becomes more and more difficult as the carbon

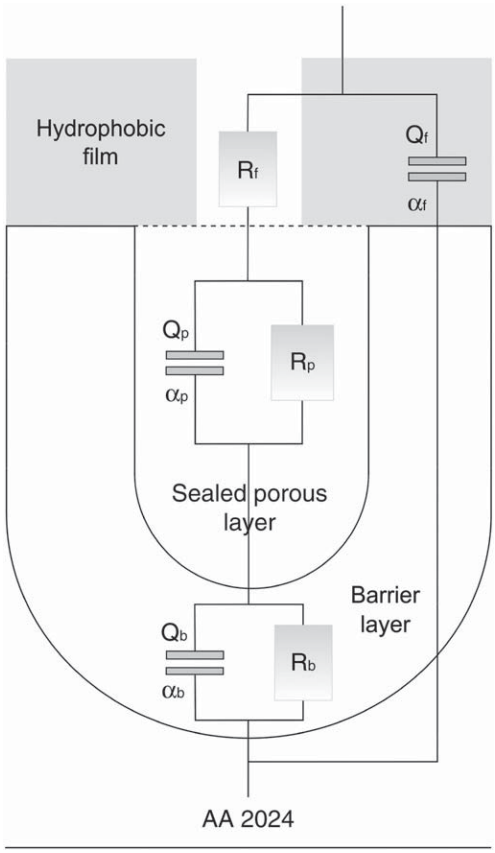

Fig. 7. Equivalent circuit used to model the impedance diagrams of the post-treated sealed anodic layers (R_f: electrolyte resistance in the pores of the organic film/Q_f and α_f: CPE parameters associated to the organic film/R_p: porous layer resistance/Q_p and α_p: CPE parameters associated to the sealed porous layer/R_b: barrier layer resistance/Q_b and α_b: CPE parameters associated to the barrier layer).

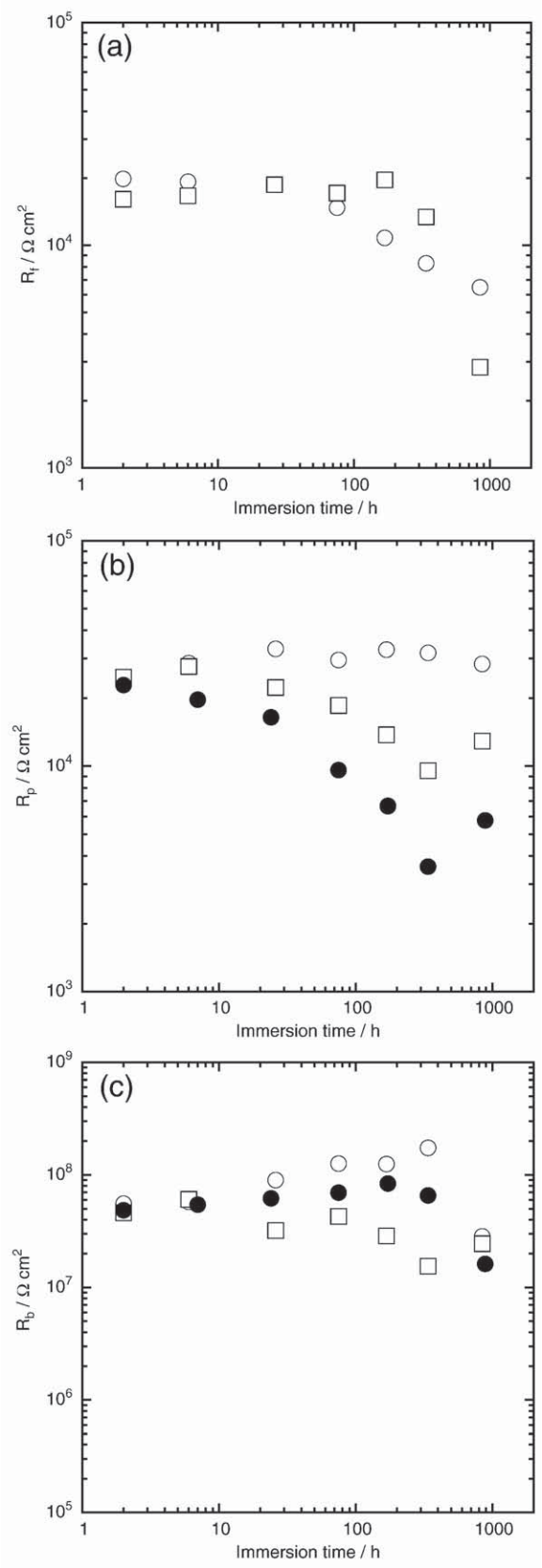

Fig. 8. (a) R_f, (b) R_p and (c) R_b values versus time of exposure to a 0.5 M NaCl solution obtained for the sealed anodic layers (●) untreated or treated at 75 °C in pure molten stearic acid for (□) 5 min and (○) 60 min.

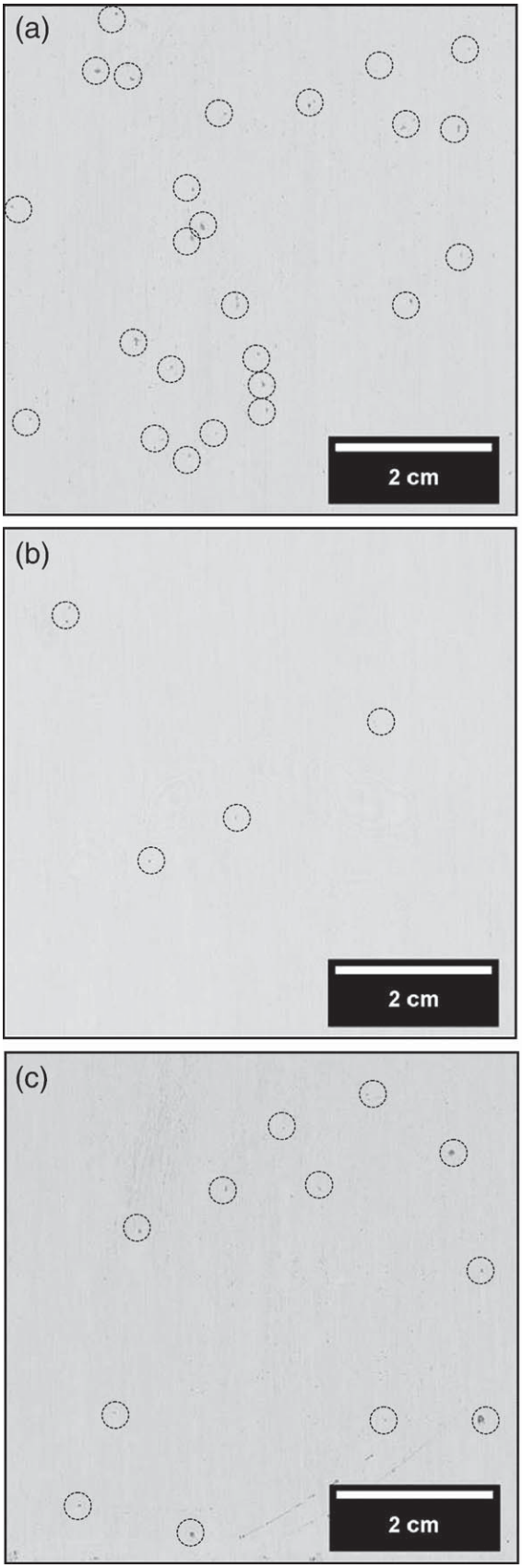

Fig. 9. Salt spray test results obtained after (a,b) 336 h and (c) 672 h for sealed specimens (a) untreated and (b,c) post-treated for 30 min at 75 °C in pure molten stearic acid. Pits have been ringed for clarity.

chain length increases. Thus, on the basis of the impedance results obtained on the unsealed anodic layers, stearic acid, with the longest carbon chain, appeared to provide the most efficient barrier.

3.4. Influence of the post-treatment time

To determine the optimal time of treatment, sealed specimens were immersed in a bath containing pure molten stearic acid at 75 °C for 5, 10, 20, 30 and 60 min. Fig. 5 presents the contact angles measured on the surface of the post-treated specimens. It appears that there is no significant variation of the hydrophobic character of the surface with the post-treatment time. Nevertheless, it can be noted that less than 5 min are necessary to obtain a hydrophobic film which indicates that the reaction involved in the post-treatment is rapid.

To better evaluate the influence of the post-treatment duration on the protective properties of the samples, EIS measurements were performed on the sealed specimens treated for 5 min and 60 min in pure molten stearic acid at 75 °C. Only these two systems were investigated to exacerbate any differences. The corrosion behaviour of the specimens was studied in a 0.5 M NaCl solution, at different exposure times reaching 35 days (840 h). Fig. 6 shows, as an example, the impedance diagrams obtained after 2 h and 336 h of immersion in a 0.5 M NaCl solution for the sealed anodic layers post-treated for 60 min in pure molten stearic acid. The plots for 5 min post-treatment were almost identical. The diagrams are characterized by three time constants. The first one in the high-frequency range concerns the protective film formed by the carboxylic acid. The second and the third time constants in the medium and high frequency ranges concern the hydrothermally sealed porous layer and the barrier layer properties, respectively. The equivalent circuit presented in Fig. 7, with three time constants, was used to fit the impedance data. The same equivalent circuit without R_f, Q_f and α_f (two time constants) was previously used to analyse the impedance data on sealed anodised AA2024 [21]. In the present study, C_{pw} (capacitance of the pore wall) was not taken into account because C_{pw} is in series with C_f (film capacitance). The value of C_f (μF) is significantly higher than C_{pw} (nF) and in the equivalent circuit, C_{pw} can be ignored.

To clearly show the presence of the hydrophobic film on the impedance spectra, they were fitted with or without the parameters associated to the hydrophobic film. The results presented in Fig. 6 show that the circuit with the three time constants gave the best fits confirming the presence of the hydrophobic film. Fig. 8 compares the variation of R_f, R_p and R_b as a function of the immersion time in the NaCl solution for the sealed specimens treated for 5 min and 60 min in pure molten stearic acid (75 °C). In Fig. 8a, it can be seen that during the first 96 h of immersion, independently of the post-treatment time, the R_f values are relatively constant and similar ($2\ 10^4\ \Omega\ cm^2$). Then, the resistances diminish. However, the decrease of R_f obtained for the sealed specimens treated for 5 min appeared to be sharper. It seems that the film formed on the sealed specimens treated for 60 min is more resistant to electrolyte penetration and chloride attack. The variation of R_p corroborates these assumptions (Fig. 8b). Indeed, the R_p values obtained for the sealed specimens treated for 60 min are constant ($3\ 10^4\ \Omega\ cm^2$) during the whole immersion time in the chloride solution. This indicates that the sealed porous layer is not deteriorated due to the efficient protection of the film which prevents electrolyte penetration. In contrast, the R_p values obtained for the sealed specimens treated for 5 min progressively decrease with the immersion time, in the same manner as the untreated specimen, revealing the degradation of the sealed porous layer. However, the values remain slightly higher than those measured on the untreated specimen. Despite the fact that the previous results showed that the formation of the coating is rapid, a longer post-treatment time improved the protection. The barrier layer resistances, R_b, remained constant versus immersion time (Fig. 8c) for the two post-treated specimens. The values were always higher than $10^7\ \Omega\ cm^2$, indicating

that the barrier layers were not attacked by the chloride ions during the whole immersion time. From the impedance results obtained in an aggressive solution, it can be concluded that the post-treatment by stearic acid improved the corrosion resistance of sealed anodised AA2024. After only 5 min of post-treatment, an improvement of the corrosion resistance can be noted and this was further enhanced by a longer post-treatment time. This enhancement of corrosion resistance is associated to the presence of the hydrophobic film ($R_f > 10^3\ \Omega\ cm^2$) which protects the porous layer from the chloride attack (R_p values are always higher with the post-treatment compared with those measured without the post-treatment) and as a consequence the degradation of the barrier layer is limited. If the barrier layer remains undamaged, the protection will be durable.

3.5. Salt spray test

To correlate the trends deduced from EIS measurements with the corrosion resistance properties, salt spray tests were performed on sealed specimens treated with the four carboxylic acids. The results showed a significant enhancement of salt spray resistance compared to non-post-treated sealed specimens, particularly for acids where $n > 4$. The best result was obtained with the stearic acid which corroborated the previous EIS measurements. As an example, Fig. 9 presents the photographs of the surfaces obtained after the salt spray test for sealed specimens before (Fig. 9a) and after post-treatment with stearic acid (Fig. 9b and c). After 336 h of salt spray exposure, the surface of the untreated specimen presents numerous pits (Fig. 9a). For the same exposure time, the surface of the post-treated specimen is practically exempt of pits (Fig. 9b); after 672 h of exposure (Fig. 9c) the surface reveals additional pits but the degradation is lower than that observed on the untreated specimen (Fig. 9a). These results clearly show the increase, in terms of corrosion resistance, afforded by the hydrophobic film formed, particularly with stearic acid, on the surfaces of the sealed specimens.

4. Conclusion

The present study highlights the promising results obtained with long-carbon-chain carboxylic acids used in the post-treatment of hydrothermally sealed AA2024 anodic layers formed in tartaric–sulphuric acid. The formation of aluminium soap conferred hydrophobic properties to the surface and thus provided a protective action which was clearly revealed by a significant enhancement of the salt spray test resistance compared to untreated specimens. The following major points emerged:

1- The post-treatment required the use of carboxylic acids in their pure molten state to allow the formation of a film with optimal hydrophobic properties.
2- Stearic acid was the most efficient of those tested. This was attributed to its longer carbon chain.
3- The organic film formed rapidly (under 5 min) but a longer time improved the corrosion protection of the sealed anodic layers.

Finally the present study showed that the post-treatment proposed is promising but some points require further investigation. For example, the carboxylic acid bath was prone to ageing (pollution, oxidation, etc.) which limits its durability. Moreover, the removal of excess acid after immersion needs to be optimised since rinsing the surface with ethanol is not suitable for industrial-scale operations.

Acknowledgments

This work was carried out with the technical and financial support of the Délégation Générale pour l'Armement and the European Aeronautic Defence and Space Company. In addition, thanks are due to D. Oquab and Y. Thebault for time on the JEOL JSM 6700F FE-SEM instrument.

References

[1] V. Moutarlier, M.P. Gigandet, L. Ricq, J. Pagetti, Appl. Surf. Sci. 183 (2001) 1.
[2] V. Moutarlier, M.P. Gigandet, J. Pagetti, B. Normand, Surf. Coat. Technol. 161 (2002) 267.
[3] G.E. Thompson, L. Zhang, C.J.E. Smith, P. Skeldon, Corrosion 55 (1999) 1052.
[4] L. Domingues, J.C.S. Fernandes, M. Da Cunha Belo, M.G.S. Ferreira, L. Guerra-Rosa, Corros. Sci. 45 (2003) 149.
[5] G.W. Critchlow, K.A. Yendall, D. Bahrani, A. Quinn, F. Andrews, Int. J. Adhes. Adhes. 26 (2006) 419.
[6] A. Dattilo, S. Tamiro, C.A. Romano, European Patent: EP1 233 084 A2 (2002).
[7] F. Mansfeld, C. Chen, C.B. Breslin, D. Dull, J. Electrochem. Soc. 145 (1998) 2792.
[8] L. Hao, B.R. Cheng, Met. Finish. 98 (2000) 8.
[9] A. Bautista, J.A. Gonzalez, V. Lopez, Surf. Coat. Technol. 154 (2000) 49.
[10] C. Rapin, A. D'Huysser, J.P. Labbe, L. Gengembre, P. Steinmetz, Rev. Métall. 93 (1996) 719.
[11] E. Rocca, J. Steinmetz, Corros. Sci. 43 (2001) 891.
[12] A. Mercer, 5th European Symposium on Corrosion Inhibitors, vol. 2, 1980, p. 563.
[13] G. Hefter, N. North, S. Tan, Corrosion 53 (1997) 657.
[14] U. Rammelt, S. Köhler, G. Reinhard, Electrochim. Acta 53 (2008) 6968.
[15] I. Raspini, Corrosion 49 (1993) 821.
[16] D. Daloz, C. Rapin, P. Steinmetz, G. Michot, Corrosion 54 (1998) 444.
[17] E. McCafferty, J.P. Wightman, J. Colloid Interface Sci. 194 (1997) 344.
[18] E. McCafferty, Corros. Sci. 45 (2003) 1421.
[19] C.C. Landry, N. Pappé, M.R. Mason, A.W. Apblett, A.N. Tyler, A.N. Maclnnes, A.R. Barron, J. Mater. Chem. 5 (1995) 331.
[20] G.P. Shulman, A.J. Bauman, Met. Finish. 93 (1995) 16.
[21] G. Boisier, N. Pébère, C. Druez, M. Villatte, S. Suel, J. Electrochem. Soc. 155 (2008) C521.
[22] T.P. Hoar, G.C. Wood, Electrochim. Acta 7 (1962) 333.
[23] J. Hitzig, K. Juettner, W.J. Lorenz, W. Paatsch, J. Electrochem. Soc. 133 (1986) 887.
[24] F. Mansfeld, M.W. Kendig, J. Electrochem. Soc. 135 (1988) 828.
[25] N. Celati, M.C. Sainte Catherine, M. Keddam, H. Takenouti, Mater. Sci. Forum 192 (1995) 335.
[26] V. López, E. Otero, A. Bautista, J.A. González, Surf. Coat. Technol. 124 (2000) 76.
[27] V. López, J.A. González, E. Otero, E. Escudero, M. Morcillo, J.A. González, Surf. Coat. Technol. 153 (2002) 235.
[28] F. Snogan, C. Blanc, G. Mankowski, N. Pébère, Surf. Coat. Technol. 154 (2002) 94.
[29] L. Domingues, J.C.S. Fernandes, M. Da Cunha Belo, M.G.S. Ferreira, L. Guerra-Rosa, Corros. Sci. 45, 149 (2003).
[30] V. Marzocchi, L. Iglesias-Rubianes, G.E. Thompson, F. Bellucci, Corros. Rev. 25, 461 (2007).
[31] V. Lopez, M.J. Bartolomé, E. Escudero, E. Otero, J.A. González, J. Electrochem. Soc. 153, B75 (2006).
[32] K. Wefers, Aluminium 49 (1973) 553.
[33] K. Wefers, Aluminium 49 (1973) 622.
[34] G.J. Brug, A.L.G. Van Den Eeden, M. Sluyters-Rehbach, J.H. Sluyters, J. Electroanal. Chem. Interfacial Electrochem. 176 (1984) 275.